WPMAT-PR(17) 17146

E. Tejado et al.

New WC-Cu thermal barriers for fusion applications: high temperature mechanical behaviour

Preprint of Paper to be submitted for publication in
Journal of Nuclear Materials

New WC-Cu thermal barriers for fusion applications: high temperature mechanical behaviour

E. Tejado[1], M. Dias[2], J.B. Correia[3], T. Palacios[1],

P.A. Carvalho[2,4], E. Alves[2], J.Y. Pastor[1]

[1] Departamento de Ciencia de Materiales-CIME,
Universidad Politécnica de Madrid, c/ Profesor Aranguren 3, E28040-Madrid, Spain.

[2] Instituto de Plasmas e Fusão Nuclear, Instituto Superior Técnico,
Universidade de Lisboa, Av. Rovisco Pais, 1049-001, Lisboa, Portugal.

[3] LNEG, Laboratório Nacional de Energia e Geologia,
Estrada do Paço do Lumiar, 1649-038 Lisboa, Portugal.

[4] CEFEMA, Instituto Superior Técnico,
Universidade de Lisboa, Av. Rovisco Pais, 1049-001 Lisboa, Portugal.

CORRESPONDING AUTHOR:
Elena Tejado
Departamento de Ciencia de Materiales-CIME, Universidad Politécnica de Madrid, c/ Profesor Aranguren 3, *E28040*-Madrid, Spain.
Telephone: +34 913365243
Email: elena.tejado@upm.es

Abstract

The combination of tungsten carbide and copper as a thermal barrier could effectively reduce the thermal mismatch between tungsten and copper alloy, which are proposed as base armour and heat sink, respectively, in the divertor of future fusion reactors.

Hence, the aim of this work is to study the thermo-mechanical properties of WC-Cu cermets fabricated by hot pressing. Focus is placed on the temperature effect and composition dependence, as the volume fraction of copper varies from 25 to 50 and 75 vol.%. To explore this behaviour, fracture experiments are performed within a temperature range from room temperature to 800 ºC under vacuum. In addition, elastic modulus and thermal expansion coefficient are estimated from these tests.

Results reveal a strong dependence of the performance on temperature and on the volume fraction of copper and, surprisingly, a slight percent of Cu (25 vol. %) can effectively reduce the large difference in thermal expansion between tungsten and copper alloy, which is a critical point for in service applications.

Keywords: WC-Cu cermet, thermal barrier, mechanical properties, thermal properties.

1. Introduction

Carbide cermets have historically been developed to provide protection against corrosion and erosion for applications in oil and gas industry, but also against heat as Thermal Barrier (TBs) to control the heat flow and retard rapid chilling. For instance, TBs have the capability to improve the durability of engines by reducing the surface temperature of the underlying components [1] . This aspect could be of great importance for future fusion power plants, where the adequate control of the heat exhaust is presently being explored [2].

One of the proposed design models of the divertor for these fusion devices is based on a structure consisting of tungsten armour and CuCrZr alloy heat sink. But the thermal expansion mismatch between these materials, together with the loss of strength and creep of CuCrZr at temperatures above 300 ºC, limit the operation temperature window of the reactor [3]. The use of a TB, along with internal cooling of the underlying plasma-facing components (PFCs), could enable the reactor to operate at higher temperatures thus achieving a remarkable increase in the efficiency and performance of the fusion plant.

This TB should withstand the harsh environment coupled with high temperature, large temperature gradient, complex stress condition and radiation [4], whilst being chemically compatible with the PFC. No single component is able to satisfy these multifunctional requirements. Nevertheless, WC-based cermets can fulfil most of the requests by the reinforcement of a metal matrix like copper. Research performed by M. Dias *et al.* found that the thermal diffusivity of cupper can be reduced by a factor of three with the addition of just 25 vol.% WC, being lower than for pure copper or tungsten, as desirable for thermal barrier materials [5]. Therefore, the thermophysical and strength properties of these materials are of great importance in order to assess their feasibility as TB.

For this purpose, the present paper presents the results on the mechanical characterization of these novel WC-Cu cermets. Focus is placed on the temperature effect and composition dependence, as the volume fraction of Cu varies from 25 to 50 and 75 %.

2. Materials and Methods

2.1. Materials

The cermets characterized in the present investigation were produced by turbular blending (1h) of commercially pure WC powder (diameter of 1 μm and 99.9% nominal purity) with Cu powder (diameter < 37 μm and 99.99% nominal purity) for variable volume fraction of Cu (25%, 50% and 75%) and subsequently consolidating the mixtures by hot pressing. Furthermore, in order to obtain the highest densification, the processing parameters (Temperature, Pressure and Time) were individually set for each composition, as presented in Table 1. Further details on the manufacturing route can be found in [5].

Table 1. Main processing parameters of the consolidated cermets.

Processing parameters	75WC-25Cu	50WC-50Cu	25WC-75Cu
Temperature (ºC)	1150	1050	900
Pressure (MPa)	47	37	22
Time (min)	6	5	5

2.2. *Characterization*

The flexural strength was tested in three-point bending (TPB) configuration on 27.0 mm× 3.5 mm× 1.3 mm bars with a crosshead speed of 100 µm/min. The reported flexural strength was the average of at least two measurements. This test configuration was also used to determine the fracture toughness (K_{IC}) of the cermets by introducing a femto-laser notch in the bottom of the bars in Single-Edge-Laser-Notched-Beam (SELNB) configuration, as explained in [6]. The stress intensity factor for mode I stress was then computed from the critical load (P_Q) and the beam section using the equation proposed by Guinea *et al.* [7]. The ASTM 5% secant method, i.e. a secant line with a slope equal to 95% of the initial elastic loading slope of the tangent line, was used to determine P_Q with an intention to define the K_{IC} at the 2 % or less crack extension [8].

Both properties were conducted at room temperature (RT), 425, 550 and 675 ºC using inductive heating at a heating rate of 10 ºC/min under very high vacuum atmosphere (10^{-6} mBar). The upper limit for test temperatures was set in 675 ºC for samples containing 50 vol. % Cu and 75 vol. % Cu due to softening of Cu at higher temperatures.

Load-deflection curves of the bending tests were used to calculate the modulus of elasticity by drawing a tangent to the steepest initial straight-line portion of it. Those data were then compared with values measured using resonance frequency analysis

(RFA) at RT. Additionally, the evolution of elastic modulus with temperature was estimated with three micromechanical models: Voigt [9], Reuss [10] and Hill [11]. Voigt model is also known as the rule of mixtures or the isostrain model, i.e. an arithmetic average of the modulus of the two components, while the Reuss model is known as the inverse rule of mixture model or the isostress model, i.e. the harmonic mean [12] . Alternatively, the Hill approach (Voigt-Reuss-Hill model, VRH) is an average of the two previous, where the loading is intermediate between the two extreme cases. Hence, the relations between volume fraction and modulus of elasticity, denoted by f and E, respectively, are the following:

$$\text{Voigt model: } E^{V}_{WC/Cu}=f\,\mathrm{WC}\ \ \mathrm{E\,WC}+f\,\mathrm{Cu\,E\,Cu} \qquad (1)$$

$$\text{Reuss model: } E^{R}_{WC/Cu}=\frac{E_{WC}\,E_{Cu}}{f\,\mathrm{Cu}\ \ \mathrm{E\,WC}+f\,\mathrm{WC\,E\,Cu}} \qquad (2)$$

$$\text{Hill model: } E^{H}_{WC/Cu}=\frac{E^{V}_{WC/Cu}+E^{R}_{WC/Cu}}{2} \qquad (3)$$

where $f_{Cu}=1-f_{WC}$

Materials data for the modulus of elasticity of WC and Cu were taken from [13] and [14], respectively.

From the above results, it was also possible to estimate the uniaxial thermal expansion coefficient, α, of the cermets, which is a relevant parameter for structural design of elements. It is well known that both properties, thermal expansion and elastic constants, are related intimately to lattice vibration, hence to the nonlinear terms in the interatomic force laws. Research performed by Barker [15] found that a large number of polycrystalline and amorphous materials obey the relation $\alpha^{s}E=15$ [N.m^{-2}.K^{-2}] at normal temperatures, where *s* is a dimensionless spread factor ($0.5<s<2$) and *E* is the elastic modulus. A later review by Arenz [16] proposed the empirical relation $E=4.5\alpha^{-2.3}$; here energy well theory and thermodynamic analysis are employed to show the qualitative relationship. Thermal expansion coefficient of the cermets was calculated with the aforementioned equation.

Finally, the microstructure and fractography were characterized by field emission scanning electron microscopy (FESEM). Chemical compositions and distribution of the elements in the cermets were determined by energy-dispersive X-ray spectroscopy (EDX) attached in the FESEM, and are shown in detail in a previous paper [5].

3. Results and discussion

Fig. 1 shows the flexural strength of the WC-Cu composites at 0.2 % plastic strain, i.e. yield strength. When fracture strain was limited to the linear elastic regime, ultimate flexural strength was reported with square symbols and dashed lines. The flexural strength, both ultimate and yield, increases with WC content, and reaches a maximum of about 800 MPa at 425 ºC, when Cu content is just 25%. Furthermore, the tensile behaviours of all three kinds of the composites exhibit almost the same trend: it reaches a maximum at 425 ºC and decreases slowly up to 675/800 ºC, with a slight recovery of the values at 675 ºC. Above this temperature, the softening of the metal phase leads to acutely low values of flexural strength, so only WC-rich composite (25 vol. % Cu) was tested under this condition.

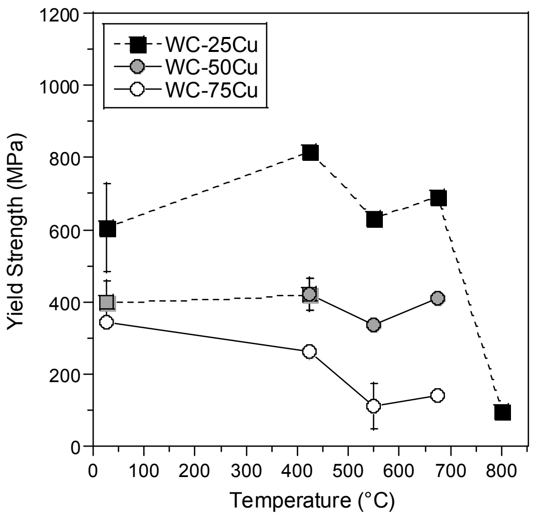

Fig. 1. Flexural strength of WC–Cu cermets as a function of composition and temperature. Mean values and standard error. Square symbols and dashed lines illustrate brittle behavior and hence, ultimate flexural strength instead of yield strength.

It is noticeable that the addition of Cu leads to a significant increase in ductility. This can be better observed in Fig. 2, where the tensile stress–strain curves of the cermets are plotted. WC-25Cu composite exhibits elastic behavior up to fracture at all temperatures, though slight plastic yield takes place at 675 ºC, which indicates that fracture is dominated by the brittle WC phase. On the contrary, the Cu-rich cermet (75 vol. % Cu) exhibits ductile behavior from RT (Fig. 4). At this temperature, the elongation is indeed one order of magnitude higher than the one exhibited by WC-25Cu. However, the rupture strength at all temperatures was considerably lower compared to the latter (700 MPa against 175 MPa at 675 ºC for WC-25Cu and WC-75Cu, respectively).

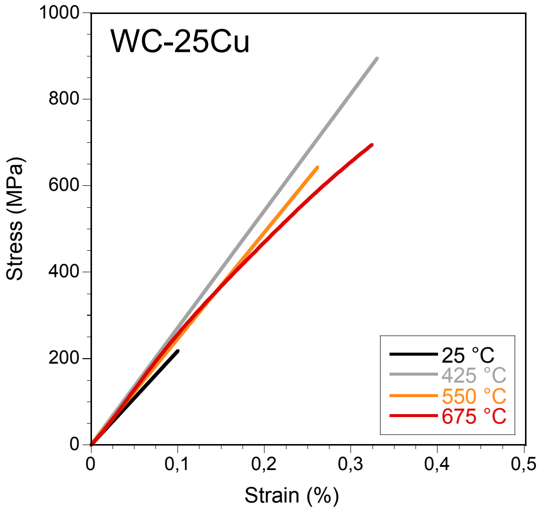

Fig. 2. Tensile curves of WC-25Cu (Cu content: 25 vol. %) at four testing temperatures.

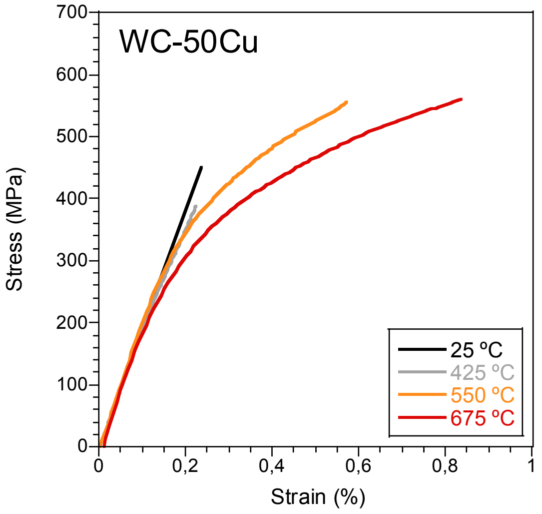

Fig. 3. Tensile curves of WC-50Cu (Cu content: 50 vol. %) at four testing temperatures.

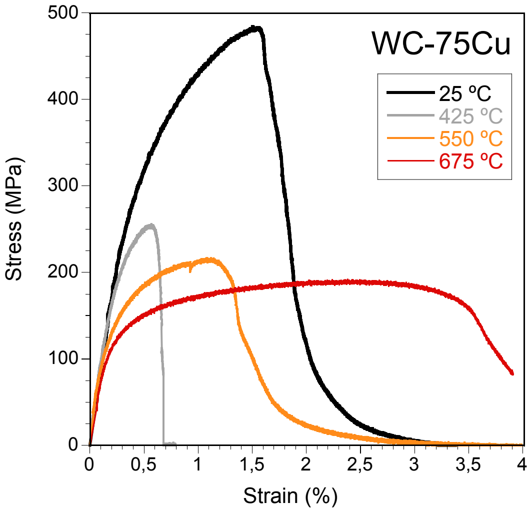

Fig. 4. Tensile curves of WC-75Cu (Cu content: 75 vol. %) with at four testing temperatures.

In Fig. 3, the tensile curves of WC-50Cu are presented. It exhibits an intermediate behavior; while rupture strains are much lower than for the Cu-rich cermet, both yield and ultimate tensile values are around 30% higher. Nevertheless, the increase in tensile elongation as compared to WC-25Cu is only evident up to 425 ºC, since both cermets present similar values of rupture strain below this temperature (< 0.3 %).

The elastic modulus values are plotted in Fig. 5 as a function of temperature and Cu content. The data were measured from the tensile curves up to 675 – 800 ºC and, additionally, at RT by means of Resonant Frequency Analysis. The elastic modulus data measured for all the cermets are located within the boundaries stablished by Voigt and Reuss, according to Eq. 1 and 2. Hill average modulus is also shown.

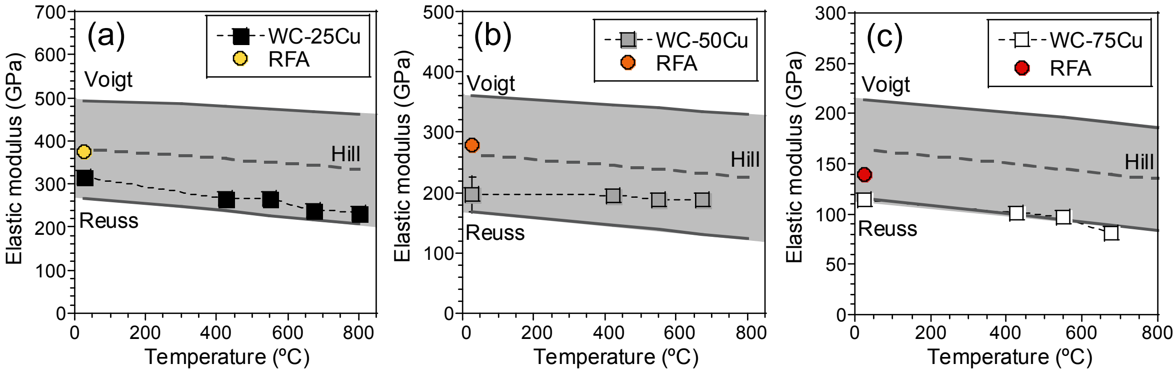

Fig. 5. Elastic modulus of a) WC-25Cu, b)WC-50Cu and c)WC-75Cu as a function of temperature, mean and standard error. Values were measured from the tensile curves and by Resonant Frequency Analysis (RFA). Upper and lower bounds were estimated with the Voigt and Reuss models, respectively, while Hill model is the average of them.

The Voigt method clearly overestimates the stiffness while the Reuss method slightly underestimates it. In all cases, the experimental values lie between Hill average and Reuss bound which seems to be a good approximation for the macroscopic constant of the cermets. However, for WC-75Cu, the results approximate Reuss values at all temperatures. This deviation of the elastic modulus to the lower bond has already been observed in particle-reinforced metallic composites, such as Cu-W [17] or Al-Cr, and it is due to a certain amount of hydrostatic stress generated in the composite when the softer matrix phase is restrained from deformation by the hard particles [18].

In order to include the effects due to porosity differences in the elastic modulus estimations, Voigt and Reuss boundaries were corrected according to the measured porosity values. Hence, no overestimation of the elastic constants has been done.

Elastic modulus values obtained from RFA are significantly higher than those measured by TPB for each cermet sample. The difference found between the stiffness obtained with dynamic and the static methods is a frequent observation and, indeed, it has been previously studied by other authors reporting this mismatch [19,20]. It is caused mainly by the fact that the dynamic modulus was derived on the basis of the material being ideal on the macroscopic level, i.e. isotropic, homogeneous and elastic. Nevertheless, Cu presents a large crystallographic anisotropy in Young´s modulus [21], and small inhomogeneities, i.e. pores or microcracks, could be neglected by the sensor. Furthermore, this technique is very sensitive to variations in dimensions of the samples [22]. Thus, a non-prismatic shape or a rough surface would lead to incorrect values of the elastic constants.

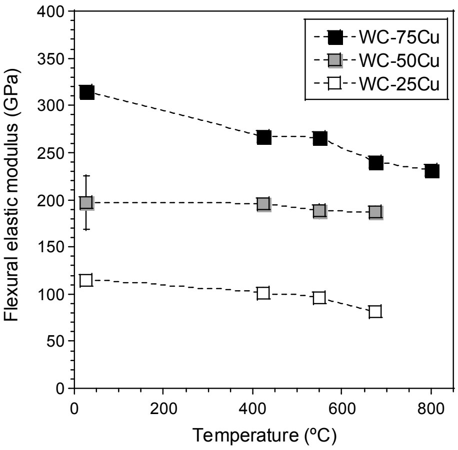

Fig. 6. Flexural elastic modulus of WC–Cu cermets as a function of composition and temperature. Mean values and standard error.

Static elastic modulus are also plotted in Fig. 6 as a function of temperature and composition. Measured stiffness is in good agreement with theoretical values, while data obtained for WC-75Cu and WC-25Cu composites follows the same trend, WC-50Cu elastic properties remain nearly constant in the temperature range tested.

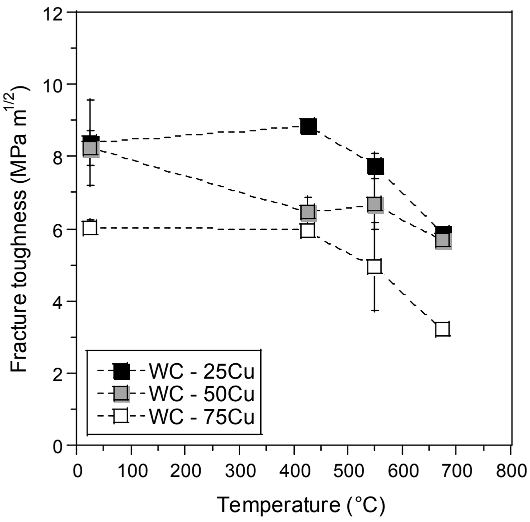

Fig. 7. Fracture toughness of the cermets as a function of temperature and composition. Mean values and standard error.

The fracture toughness results of WC-Cu cermets as a function of temperature are shown in Fig. 7. It can been observed that there is an improvement in the fracture toughness when the WC volume fraction increases from 25 to 75 vol. %. In addition, a clear trend with temperature can be inferred from it. At RT, where little plastic deformation is observed, both WC-25Cu and WC-50Cu composites exhibit toughness around 8 MPa m$^{1/2}$. On the contrary, when temperature increases, the effect of the high concentration of WC is more evident, showing the highest value of toughness, ~ 9 MPa m$^{1/2}$ at 425 ºC for W-75Cu. This effect has already been observed for W-based materials [23], and it is due to a softening of the grain boundaries and explained by the blunting of the crack tip [24]. Up to this temperature, Cu ductile phase controls the fracture and, hence, the degradation of the cermet.

The difference in properties of the three materials is evident upon viewing their fracture surfaces. Fig. 8(a) shows a micrograph of the WC-rich cermet (25 vol. % Cu) that justifies the macroscopic brittle fracture at all the temperatures tested. The carbide particles evidence flat, cleaved planes, while the microstructural ductile nature of the Cu phase results in the elongation of the metal around the carbide particles. This effect is more pronounced when the Cu content in the cermets is increased (Figure 8 (b)and (c)). Fig. 9 shows the residual porosity present after material processing. Nevertheless, in spite of the thermal mismatch and the weak bond between WC and Cu, since no decohesion was observed between both phases.

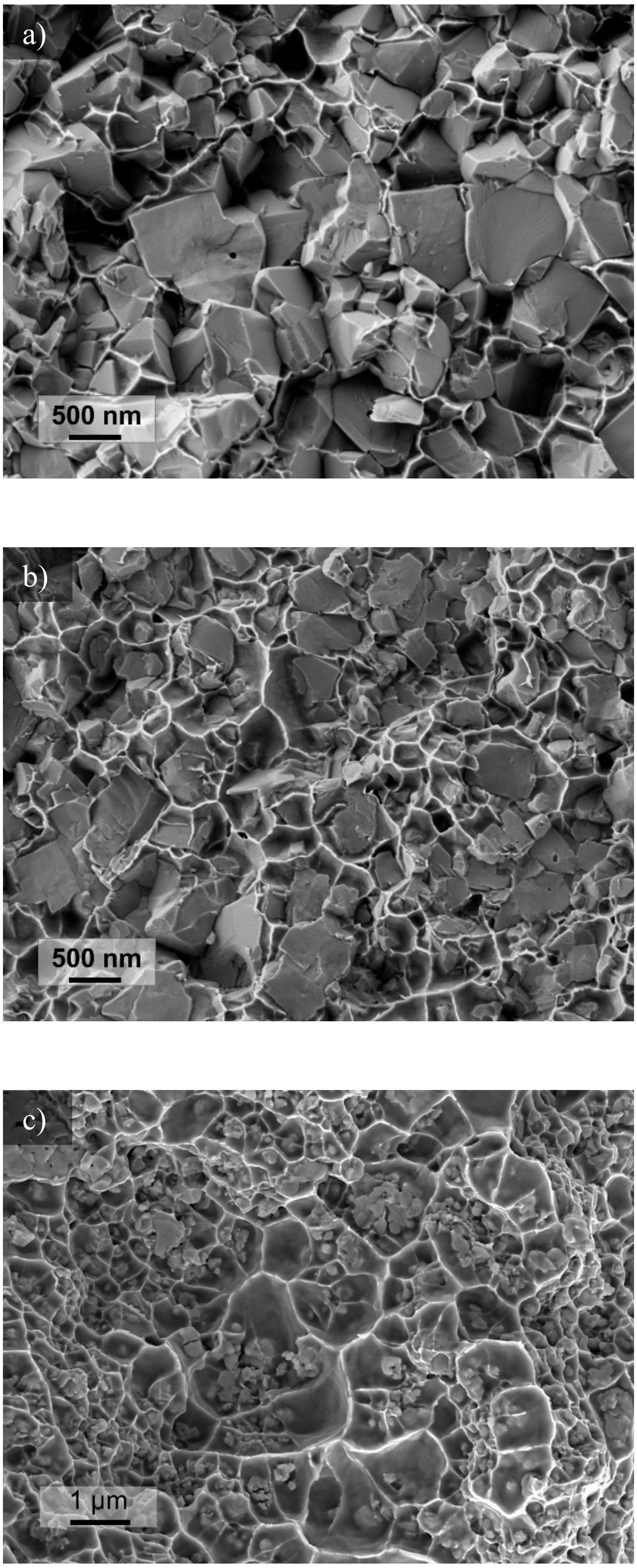

Fig. 8. Fractographs of WC–Cu cermets tested at 25 ºC: a) WC-25 vol. % Cu, b) WC-50 vol. % Cu and c) WC-75 vol. % Cu.

The dominant modes of fracture can be observed in Fig. 8(b): transgranular fracture of WC particles and plastic deformation of Cu matrix. The number of fracture dimples is relatively lower (see Figure 8(a)) and increases gradually with the Cu volume fraction in the WC-Cu system. Transgranular fracture of WC particles can be explained by the existence of cracks that can be propagated from stress concentrators, i.e. pores and defects observed in Fig. 8(a), along the crystal planes during fracture process.

The degradation of the tensile performance up to 425 ºC can be explained through Fig. 9 that shows the fractography of a WC-rich (75 vol. % Cu) sample tested at 675 ºC. While WC particles remain practically unaltered, Cu phase is clearly degraded because of the temperature increase. This image illustrates as well inhomogeneities in the grain size of WC particles which could be the reason of the no so high performance of WC-25Cu composite as expected.

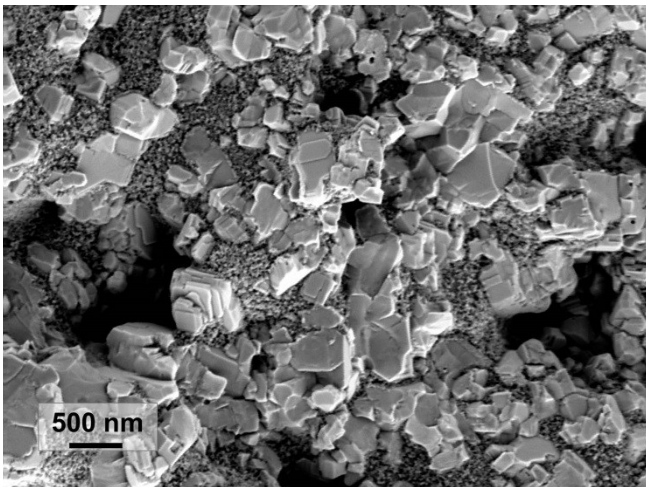

Fig. 9. Fractograph of WC–75Cu cermet tested at 675 ºC in vacuum.

Fig. 10 shows the coefficient of thermal expansion of the WC-Cu composites between RT and 800 ℃. It can be observed that an increase in Cu leads to an increase in this coefficient. Furthermore, this effect is more evident at higher temperatures. Nevertheless, these data has been obtained from the empirical relation $\alpha^{s}E=15$ (N m^{-2} K^{-}

^{2}), where *E* is the elastic modulus measured from the bending tests (see Fig. 6). In order to analyse their suitability as thermal barriers for fusion applications, literature values of W and CuCrZr have been represented in Fig. 10. It can be observed that, with just a small percent of Cu, these cermets can reduce the thermal expansion coefficients mismatch between W and CuCrZr and, therefore, they are effective as thermal barriers.

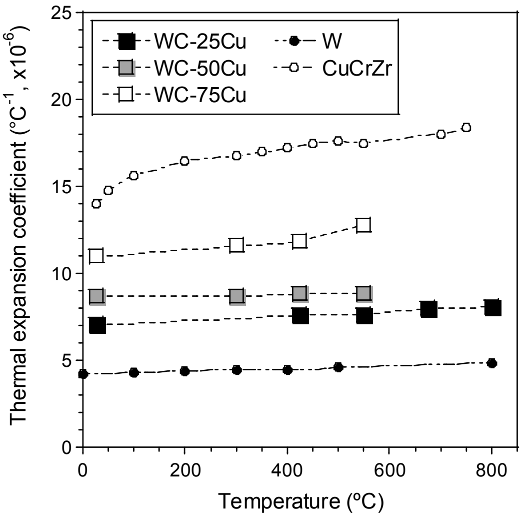

Fig. 10. Coefficient of thermal expansion of the WC-Cu cermets as a function of composition and temperature. Literature values for CuCrZr [25] and W [26] are also presented.

4. Conclusions

The effect of Cu on thermal and mechanical properties of WC-Cu cermets was studied. Three compositions (25, 50 and 75 vol. percentage of Cu) were tested up to 800 ºC (WC-75Cu) and 675 ºC (WC-50Cu and WC-25Cu) both under vacuum atmosphere.

Fracture surfaces of WC-Cu composites revealed two kinds of fracture mechanisms: transgranular cleavage of WC particles and ductility of Cu phase. The dominant fracture mechanism depends strongly on the content of Cu and temperature, hence macroscopic ductile behavior and high rupture strains were observed for Cu-rich cermet (75 vol. % Cu).

On the contrary, the tensile behavior of WC-25Cu was brittle up to fracture and up to 675 ºC, where slight plastic yield appears. In addition, the high concentration of WC resulted on the highest values of tensile strength at 425 ºC, 800 MPa. The behavior of WC-50Cu cermet is in-between the observed for the above cermets, with brittle to ductile transition at 425 ºC.

The measured elastic properties fit well the analytical models for composite materials, with values between the theoretical boundaries for all cases. From these results it was possible to estimate the thermal expansion coefficient of the cermets and, thereby their suitability as thermal barriers for fusion applications. Results showed that a slight percent of Cu (25 vol. %) can reduce strongly the large difference in thermal expansion between tungsten and CuCrZr as armour component and heat sink, respectively.

Acknowledgment

This work has been carried out within the framework of the EUROfusion Consortium and has received funding from the Euratom research and training programme 2014-2018 under grant agreement No 633053. The views and opinions expressed herein do not necessarily reflect those of the European Commission

The authors also acknowledge the support of the Ministerio de Economía y Competitividad of Spain (research projects MAT2012-38541-C02-02 and MAT2015-70780-C4-4-P) and the Comunidad de Madrid (research project S2013/MIT-2862-MULTIMATCHALLENGE) who have funded this research.

IST activities received financial support from Fundação para a Ciência e Tecnologia through project Pest-OE/SADG/LA0010/2013, from the Portuguese Science and Technology Foundation (FCT) under the PTDC/CTM/100163/2008 grant and the PEST-OE/CTM-UI0084/2011 contracts. M. Dias acknowledges the FCT grant SFRH/BPD/68663/2010.

References

1 []P. Fauchais and A. Vardelle. Thermal Sprayed Coatings Used Against Corrosion and Corrosive Wear, Advanced Plasma Spray Applications, Dr. Hamid Jazi (Ed.), InTech, (2012) DOI: 10.5772/34448.

2 []M. Turnyanskiy *et al*. European roadmap to the realization of fusion energy: Mission for solution on heat-exhaust systems, Fusion Eng. Des. (2015)

3 []Jeong-Ha You. Copper matrix composites as heat sink materials for water-cooled divertor target, Nuclear Materials and Energy, Volume 5, December 2015, Pages 7-18, ISSN 2352-1791.

4 []H. Xu and H. Guo. Thermal Barrier Coatings, Woodhead Publishing in Materials (2011). ISBN 978-1-84569-658-0.

5 []M. Dias, F. Guerreiro, E. Tejado, J. B. Correia, T. Palacios, J.Y. Pastor, P.A. Carvalho, E. Alves. New WC-Cu thermal barriers for fusion applications: thermal and mechanical characterization (2017)

6 []ASME B31.1-1995.

7 []G. V. Guinea, J. Y. Pastor, J. Planas and M. Elices. Stress Intensity factor, compliance and CMOD for a general three-point-bend beam. International Journal of Fracture 83: 103-116, 1998.

8 []ASTM E1820-11. Standard test method for measurement of fracture toughness. American Society for Testing and Materials; 2011

9 []W. Voigt. Uber die Beziehung zwischen den beiden Elastizitatskonstanten Isotroper Korper. Wied. Ann, 38 (1889) 573-587.

[10] []A. Reuss. Berechnung der Fliessgrense von Mischkristallen auf Grund der Plastizitätsbedingung für Einkristalle. Zeitschrift Angewandte Mathematik und Mechanik, 9 (1929) 49-58.

[11] []R. Hill. The elastic behaviour of a crystalline aggregate. Proceedings of the Physical Society. Section A 65, 349 (1952).

[12] []R. Younes, A. Hallal, F. Fardoun and F. H. Chehade. Comparative Review Study on Elastic Properties Modeling for Unidirectional Composite Materials. Intech (2012). DOI: 10.5772/50362.

[13] []J. M. Wheeler and J. Michler. Indenter materials for high temperature nanoindentation. Rev Sci Instrum. Vol. 84 (10). DOI: 10.1063/1.4824710.

[14] []ASM Specialty Handbook: Copper and Copper Alloys. J.R.Davis, editor, p430-439. (2001). ISBN: 0-87170-726-8; DOI: 10.136/caca2001p430

[15] []R. E. Jr. Barker. An Approximate Relation Between Elastic Moduli and Thermal Expansivities, Journal of Applied Physics, 34(1), 107-116, 1963.

[16] []R. J. Arenz. Relation of Elastic Modulus to Thermal Expansion Coefficient in Elastic and Viscoelastic Materials. Conference Paper 2005 SEM Annual Conference & Exposition on Experimental and Applied Mechanics.

[17] [] G. Weidmann, P. Lewis, Structural Materials, Materials in Action Series, Ed. Butterworth-Heinemann (July 1990), ISBN-13: 978-0408046589

[18] []Handbook of Aluminum: Volume 2: Alloy Production and Materials Manufacturing, Ed. G.E. Totten and D. S. MacKenzie, April 25, 2003 by CRC Press, ISBN 9780824708962.

[19] []H. Ledbetter. Dynamic vs static Young moduli: A case study. Mater. Sci. Eng., A 165(1), L9 (1993).

[20] []M. Radovic, E. Lara-Curzio and L. Riester. Comparison of different experimental techniques for determination of elastic properties of solids. Materials Science and Engineering A368 (2004) 56–70. DOI:10.1016/j.msea.2003.09.080

[21] []D.E.J. Armstrong, A.J. Wilkinson and S.G. Roberts. Measuring anisotropy in Young's modulus of copper using microcantilever testing, Journal of Materials Research, 24(11), pp. 3268–3276. DOI: 10.1557/jmr.2009.0396.

[22] []G. Quinn and J. Swab. Elastic Modulus by Resonance of Rectangular Prisms: Corrections for Edge Treatments. J. Am. Ceram. Soc. 83 (2) (2000) 317. DOI: 10.1111/j.1151-2916.2000.tb01192.x

[23] []E. Tejado, P. A. Carvalho, A. Munoz, M. Dias, J. B. Correia, U.V. Mardolcar, J. Y. Pastor. The effects of tantalum addition on the microtexture and mechanical behaviour of tungsten for ITER applications, Journal of Nuclear Materials, Volume 467, Part 2, December 2015, Pages 949-955.

[24] []J. J. Kübler. Fracture toughness of ceramics using the SEVNB method: from a preliminary study to a standard test method. In: J. A. Salem, G. D. Quinn, M. G. Jenkins, editors. Fracture resistance testing of monolithic and composite brittle materials: STP 1409. Pennsylvania: ASTM; 2002. pp. 93–106.

[25] []Y. Birol. Thermal fatigue testing of CuCrZr alloy for high temperature tooling applications, J. Mater. Sci. (2010) 45:4501–4506.

[26] []P. Hidnert, W.T. Sweeney. Thermal expansion of tungsten. National Bureau of Standards. Scientific Papers (1925).